0026-895X/03/6305-1012–1020$7.00
MOLECULAR PHARMACOLOGY
Copyright © 2003 The American Society for Pharmacology and Experimental Therapeutics
Mol Pharmacol 63:1012–1020, 2003

Vol. 63, No. 5
2190/1060485
Printed in U.S.A.

Glucocorticoid Receptor Antagonism by Cyproterone Acetate and RU486

CHRISTIAN HONER, KIYEAN NAM, CYNTHIA FINK, PAUL MARSHALL, GARY KSANDER, RICARDO E. CHATELAIN, WENDY CORNELL, RONALD STEELE, ROBERT SCHWEITZER, and CHRISTOPH SCHUMACHER

Novartis Institute for Biomedical Research, Summit, New Jersey (C.H., C.F., P.M., G.K., R.E.C., W.C., R.S., R.S., C.S.); and Graduate School of Biomedical Sciences, University of Medicine and Dentistry of New Jersey, Piscataway, New Jersey (K.N.)

Received October 2, 2002; accepted February 5, 2003

This article is available online at http://molpharm.aspetjournals.org

ABSTRACT

The steroid compound cyproterone acetate was identified in a high-throughput screen for glucocorticoid receptor (GR) binding compounds. Cyproterone (Schering AG) is clinically used as an antiandrogen for inoperable prostate cancer, virilizing syndromes in women, and the inhibition of sex drive in men. Despite its progestin properties, cyproterone shares a similar pharmacological profile with the antiprogestin mifepristone (RU486; Roussel Uclaf SA). The binding affinities of cyproterone and RU486 for the GR and progesterone receptor were similar (K_d, 15–70 nM). Both compounds were characterized as competitive antagonists of dexamethasone without intrinsic transactivating properties in rat hepatocytes (K_i, 10–30 nM). In osteosarcoma cells, RU486 revealed a higher potency than cyproterone acetate to prevent responses to dexamethasone-induced GR transactivation and NFκB transrepression. Upon administration to Sprague-Dawley rats, both compounds were found to be orally bioavailable and to inhibit transactivation of liver GR. Molecular docking of cyproterone acetate and RU486 into the homology model for the GR ligand binding domain illustrated overlapping steroid scaffolds in the binding pocket. However, in contrast to RU486, cyproterone lacks a bulky side chain at position C11β that has been proposed to trigger active antagonism of nuclear receptors by displacing the C-terminal helix of the ligand-binding domain, thereby affecting activation function 2. Cyproterone may therefore inhibit transactivation of the GR by a molecular mechanism recently described as passive antagonism. New therapeutic profiles may result from compounds designed to selectively stabilize the inactive and active conformations of certain nuclear receptors.

Glucocorticoids are steroid hormones that are essential for normal growth and development, for liver and immune functions, and for mediating the stress response. Synthetic derivatives of glucocorticoids, such as dexamethasone, have immunosuppressive, anti-inflammatory, osteocatalytic, proteolytic, and hyperglycemic activities and are used to treat various pathological conditions (Sapolsky et al., 2000). The GR is a ligand-activated intracellular transcriptional regulator that is a member of the nuclear receptor superfamily. In the absence of a ligand, the GR is retained in the cytoplasm by association with chaperone proteins. Upon ligand binding, the GR dissociates from chaperones, dimerizes, and translocates into the nucleus. In the nucleus, the hormone-bound GR can modulate transcription of target genes by direct interaction with specific DNA sequences, called glucocorticoid response elements (GRE) in GR responsive promoters (Karin, 1998). Alternatively, activated GR can interact with nuclear factor κB (NF-κB) or with activator protein 1 (AP-1) to repress gene expression induced by these proinflammatory transcription factors. The anti-inflammatory and immunesuppressive properties of glucocorticoids have been largely attributed to the transrepression of NF-κB and AP-1 function, whereas the hyperglycemic effects have been ascribed to GRE-mediated transactivation of metabolic enzymes. The recent elucidation of the GR crystal structure has demonstrated the relevance of the dimer interface for GR-mediated transactivation (Bledsoe et al., 2002). In contrast, transrepression of NF-κB and AP-1 function has been shown to be dependent on nuclear translocation yet independent of dimer formation.

Gene transactivation has been explained by a ligand-induced change in the nuclear receptor structure that allows the recruitment of a coactivator. The receptor coactivator complex is believed to acetylate histones and thus to prepare target gene promotors for transactivation by decondensation of the corresponding chromatin (McKenna et al., 1999; Bour-

This work was supported by the University of Medicine and Dentistry of New Jersey/Novartis Predoctoral Fellowship Program.

ABBREVIATIONS: GR, glucocorticoid receptor; GRE, glucocorticoid response element; NF-κB, nuclear factor κB; AP-1, activator protein 1; LBD, ligand-binding domain; AF-2, activation function 2; RU486, mifepristone; PR, progesterone receptor; DMSO, dimethyl sulfoxide; DTT, dithiothreitol; FP, fluorescence polarization; Fluormone-GS1, fluorescent glucosteroid; PL, progesterone ligand; IL, interleukin; TAT, tyrosine aminotransferase; THC, (*R*,*R*)-5,11-*cis*-diethyl-5,6,11,12-tetrahydrochrysene-2,8-diol.

guet et al., 2000; Glass and Rosenfeld, 2000). The LBDs in nuclear receptors contain, at their carboxyl-terminal ends, a helix that mediates a ligand-controlled AF-2. The LBDs derived from several nuclear receptors have been crystallized and shown to fold into a three-layer helical sandwich (Bourguet et al., 1995; Renaud et al., 1995; Wagner et al., 1995; Williams and Sigler, 1998; Sack et al., 2001). Ligands bind into a hydrophobic pocket contained in the sandwich and interact with the AF-2 helix. Ligands with transactivation or agonistic function position the AF-2 helix in an active conformation that allows the association of coactivators (Brzozowski et al., 1997). Antagonists of ligand-dependent transactivation often resemble agonists in their core scaffold with the exception of an additional extended bulky side chain. This ligand side chain has been shown to reposition the AF-2 helix within the nuclear receptor ligand binding groove and thus to switch affinity of the LBD from coactivator to corepressor recruitment (Chen and Evans, 1995).

The most widely used antiprogestin, RU486, was originally developed as an antiglucocorticoid and was subsequently shown to effectively repress GR-mediated transactivation (Philibert and Teutsch, 1990; Teutsch et al., 1991). The dimethylaminophenyl moiety of RU486 is believed to confer antagonist activity via interactions in the 11β-pocket of the progesterone receptor (PR), resulting in the inhibition of transcriptional activity (Gronemeyer et al., 1992; Cadepond et al., 1997).

In a search for new GR modulating compounds, we used a high-throughput, GR-competitive ligand-binding screen and identified a compound of unique steroidal structure. The compound GP052499 represented cyproterone acetate and was characterized as a potent GR antagonist despite the lack of any 11β-substitution.

Materials and Methods

Human Steroid Receptor Binding Assays. GR and PR competitive ligand binding assays (PanVera, Madison, WI) were adapted to a 384-well format for high-throughput screening. Both binding assays required, according to the manufacturer's protocol, the preparation of buffer, receptor, and tracer solutions in addition to the serial dilutions of test compound.

For the GR assay, the binding buffer was prepared by diluting 1 ml of the 10× stock solution [100 mM KPO_4 (K_2HPO_4 − 80.2% and KH_2PO_4 − 19.8%, pH 7.4), 100 mM Na_2MoO_4, 1 mM EDTA, and 20% DMSO] with 7.95 ml H_2O, 1 ml of a 10× stabilizing peptide (1 mM), and 50 μl of 1 M DTT. A 2.2 nM fluorescent glucosteroid (Fluormone-GS1) solution was prepared in 1× GR-binding buffer. In the binding reaction, 10 μl of the Fluormone-GS1 solution was diluted to a final volume of 22 μl, yielding a 1 nM tracer ligand concentration. The GR preparation was thawed on ice for at least 1 h before the preparation of an 8.8 nM GR solution in 1× GR-binding buffer (Srinivasan and Thompson, 1990). In the binding reaction, 10 μl of the GR solution was diluted to a final volume of 22 μl, yielding a 4.0 nM concentration of functional receptor. The ratio of 1.0 nM Fluormone-GS1 to 4.0 nM GR resulted in a receptor saturation of approximately 80%.

For the PR assay, 4.4 nM green fluorescent progesterone ligand (Fluormone-PL) solution was prepared in binding buffer containing 10% glycerol, 100 mM potassium phosphate, pH 7.4, 100 μg/ml bovine serum albumin, and 1 mM DTT. An 88 nM glutathione *S*-transferase-PR-ligand binding domain fusion protein solution was prepared in binding buffer. In the binding reaction, 10 μl of the receptor solution was diluted in a final volume of 22 μl, yielding a 40 nM receptor concentration that was saturated by approximately 80% with ligand in the presence of 2 nM Fluormone-PL.

Serial dilutions of steroid test compounds were prepared in 11-fold excess concentrations with H_2O. In the binding reactions, 2 μl of test compound solution was diluted in a final volume of 22 μl. The steroid binding assay consisted of pipetting 2 μl of ligand dilution followed by 10 μl of Fluormone-GS1 and 10 μl of GR-solution into a 384-well plate (Nalge Nunc International, Naperville, IL). Negative and positive controls were included to determine the fluorescence polarization (FP) window. The plate was incubated in the dark at room temperature for 1 h before FP analysis at 485 nm excitation and 530 nm emission using an Analyst II (Beckman Coulter, Fullerton, CA).

Statistical Evaluation of Binding Curves. The steroid concentration that resulted in a half-maximum shift in polarization equaled the IC_{50} value, a measure of the relative affinity of ligand for the receptor. The curves were plotted with the Prism software (GraphPAD, San Diego, CA) using the equation: $Y = [mP_{100\%} + (mP_{0\%} - mP_{100\%})]/(1 + 10^{[(LogIC_{50} - X) \times \text{Hill slope}]})$, where Y = mP; X = Log [ligand concentration]; $mP_{100\%}$ = mP at 100% inhibition; $mP_{0\%}$ = mP at 0% inhibition. The conversion of IC_{50} values into K_i values was calculated with the equation of Cheng and Prusoff (Cheng and Prusoff, 1973): $K_i = IC_{50}/(1 + [\text{fluormone-GS1}]/0.2\ \text{nM})$, where K_i represents the receptor affinity for the competing ligand. The subscript i was used to indicate that the competitor-inhibited tracer ligand binding was interpreted as an equilibrium dissociation constant K_d. It is the concentration of the competing ligand that will bind to half of the binding sites at equilibrium in the absence of tracer ligand. Competitor affinities (K_i values) were determined relative to tracer affinities (K_d values). The K_d value for the tracer fluormone-GS1 used was provided by the manufacturer: 0.2 nM at 4°C and 2-h incubation (PanVera, Madison, WI). To determine experimentally the K_d value for a FP-labeled tracer, a saturation titration was performed with a constant amount of fluormone-GS1 (1 nM) and serial dilutions of GR (0.01–100 nM). The equilibrium binding curve was then generated by plotting δ-FP [mP] values against free GR [nM] values.

Cellular Tyrosine Aminotransferase Activity Assay. Rat hepatoma H4IIE-C3 cells were obtained from the American Type Culture Collection (Manassas, VA) and seeded at 40,000 cells per well in a 96-well plate. The cells were cultured at 37°C in a 5% CO_2 atmosphere in 100 μl of low-glucose Dulbecco's modified Eagle's medium (Invitrogen, Carlsbad, CA) containing 10% fetal calf serum (Invitrogen) and 500 units/ml penicillin and streptomycin. After 3 days, the cells were fed with an additional 100 μl of fresh media. On the following day, media was removed, and monolayers were treated overnight with varying concentrations of dexamethasone ± 10 μM concentrations of test compounds (Schild-format) or varying concentrations of test compounds ± 10 nM dexamethasone (Titration format) in 200 μl of fresh media. After 24 h, the compound-containing media were removed, and the cell monolayers were washed once with phosphate-buffered saline. Monolayers were then treated with 50 μl of freshly prepared solubilization buffer (125 mM K_2HPO_4, pH 7.6, 1.0 mM EDTA, pH 8.0, 1.0 mM DTT, 0.5% Nonidet P-40) and placed on ice for 10 min. After solubilization, to each well was added: 130 μl L-tyrosine (8.75 mM stock; 63.125 mg in 32 ml of 125 mM K_2HPO_4 and 150 μl of 10 N KOH: final preparation performed immediately before assay by adding 0.6 ml of 125 mM KH_2PO_4 to 1.0 ml of tyrosine stock), 10 μl of pyridoxyl phosphate (1 mM stock; 4.8 mg in 10 ml of 125 mM K_2HPO_4) and 10 μl of α-ketoglutarate (200 mM stock; 368 mg in 10 ml of 125 mM K_2HPO_4 and 150 μl of 10 N KOH). Plates were then incubated for 30 min at 37°C. Reactions were stopped and final measurable components developed by the addition of 3 μl of 10 N KOH with immediate mixing after addition to each well. Plates were incubated for an additional 30 min at 37°C, transferred to a quartz 96-well plate and then read spectrophotometrically at 340 nm UV.

Statistical Evaluation of the TAT Assay. The saturation binding experiment measures steroid concentration-dependent induction of tyrosine aminotransferase (TAT) activity. The Prism software (GraphPAD, San Diego, CA) provides a logistic equation describing a

sigmoidal dose-response curve for nonlinear regression analysis: $Y = A_{min} + (A_{max} - A_{min})/(1 + X/X_o)^P$, where X represents the concentration of ligand and Y the specific activity data. With these values, an activation curve is fitted and analyzed for the EC_{50} value (X_o). A_{max} represents the plateau value of maximal effect, whereas A_{min} is the value of minimal effect. P represents the Hill slope variable that controls the slope of the curve.

Reporter Gene Assays. MG63 osteosarcoma cells were obtained from the American Type Culture Collection and transiently transfected with a pGRE-Luciferase reporter plasmid (BD Biosciences Clontech, Palo Alto, CA) at 2 μg of plasmid per million cells using LipofectAMINE 2000 reagent according to the manufacturer's instructions (Invitrogen). After an overnight transfection, the cells were replated into a 96-well plate and allowed to adhere for 8 h. The cells were then treated with test compound or vehicle control (0.1% DMSO) for 1 h before the addition of dexamethasone. On the following day, the induction of luciferase was measured using the Bright-Glo luciferase assay system (Promega, Madison, WI).

Cellular IL-6 Secretion Assay. MG63 osteosarcoma cells obtained from American Type Culture Collection were cultured at 37°C in RPMI 1640 medium and 10% fetal calf serum (Invitrogen) until reaching confluence. At confluence, the media was changed to RPMI 1640 medium and 2% fetal calf serum (charcoal-stripped). After 3 days, the cells were treated with test agents or their vehicle (0.1% DMSO) for 1 h before adding interleukin (IL)-1β at 30 ng/ml (BioSource, Camarillo, CA). After an overnight incubation, the extracellular media was assayed quantitatively for IL-6 levels using an enzyme immunoassay kit (Cayman Chemical, Ann Arbor, MI). The IL-1β stimulated cells produced 400 pg of IL-6 per 5000 cells, whereas unstimulated cells yielded <10 pg of IL-6 per 5000 cells. The results were normalized to percentage of inhibition in response to dexamethasone.

In Vivo Rat Treatment and ex Vivo Liver TAT Activity Assay. Male Sprague-Dawley rats weighing 180 to 220 g were delivered a week before the study from the Harlan Farms (Harlan Sprague-Dawley, Indianapolis, IN) and housed under standard laboratory conditions outlined by the Animal Care and Use Committee. The rats were fasted for 18 h before the start of the experimental procedure. The rats were divided into groups of four and dosed orally by gavage with either vehicle (0.25% carboxymethylcellulose in water containing 20% ethanol) or vehicle-solubilized test compound (40 or 80 mg/kg). Ten minutes after the oral gavage procedure, the rats were administered an i.p. injection of either vehicle (20% ethanol solution) or various doses of vehicle-solubilized dexamethasone (0.003, 0.01, 0.03, and 0.15 mg/kg). After the injections, the rats were sacrificed at various time points (1, 3, or 5 h) with isoflurane. The livers were removed and the periportal regions were immediately frozen in liquid nitrogen and stored at −70°C. Working on dry ice, a portion of the frozen liver was placed in 4 ml of cell solubilization buffer (0.125 M K_2HPO_4, pH 7.6, 1 mM EDTA, pH 8.0, 1 mM DTT, 0.5% Nonidet P40) and subjected to mechanical homogenization. The resultant homogenate was transferred to a 4.7-ml OptiSeal tube (Beckman Coulter, Fullerton, CA), and cytosolic fractions were obtained by ultracentrifugation at 40,000 rpm for 1 h. Supernatant, below the fat plug, was retrieved by needle and syringe and placed in a clean, sterile tube on ice. All samples were standardized for protein content at 1.0 μg/μl (Bio-Rad, Hercules, CA). Subsequently, 50 μl of the standardized cytosolic fraction was assayed for TAT activity as described previously. After addition of 130 μl of L-tyrosine solution, 10 μl of pyridoxyl phosphate solution, and 10 μl of α-ketoglutarate solution, the samples were incubated for 30 min at 37°C. The reactions were stopped and the final measurable components developed by the addition of 3 μl of 10 N KOH solution with immediate shaking after addition to each well. Plates were incubated for an additional 30 min at 37°C, transferred to a quartz 96-well plate and then read spectrophotometrically at 340 nm UV. Data points ($n = 4$) are presented as mean ± S.D. Comparisons were made using the Student's unpaired t test.

GR Homology Modeling and Ligand Docking. A pair-wise sequence alignment of the human GR-LBD (Swiss-Prot accession number P04150) and the human PR-LBD (Swiss-Prot accession number P06401) was carried out using the Smith-Waterman algorithm with a BLOSUM62 scoring matrix and default gap penalties (gap open, 10; gap extend, 0.5). The homology model for the GR-LBD was built based on the X-ray crystal structure for PR-LBD (Protein Data Base code 1A28) using the homology modeling module in the MOE program (Chemical Computing Group Inc., Montreal, ON, Canada). The LMOD (Low MODe conformation search) function (Kolossvary and Guida, 1996, 1999) in the Macromodel suite version 7.0 (Schrodinger Inc., Portland, OR) was used to dock ligands and refine structures of GR-LBD homology model.

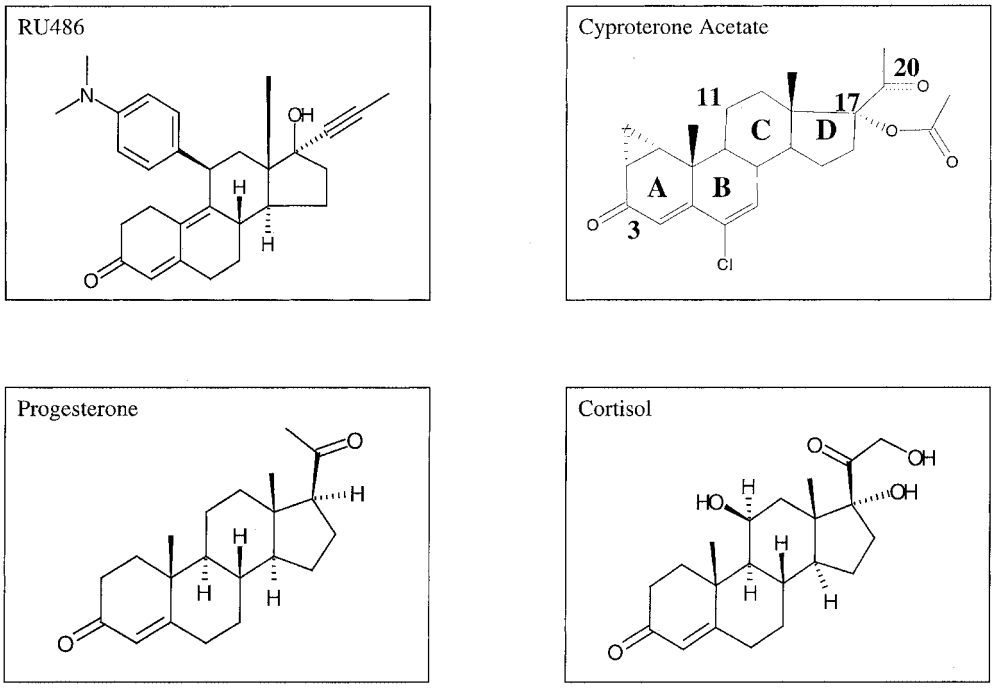

Fig. 1. Chemical structures of RU486 (mifepristone/RU38486), cyproterone acetate, progesterone, and cortisol. The steroid template of cyproterone acetate is annotated and numbered according to the IUPAC guidelines.

Results

Steroid Equilibrium Binding to the Human GR and PR. An in vitro GR competitive binding assay was established with a baculovirus derived crude human receptor preparation and a fluorescent glucocorticoid in a 384-well, high-throughput format (Srinivasan and Thompson, 1990). Dose-dependent displacement of the fluormone-labeled glucosteroid with competing compounds was recorded by fluorescence polarization. In this assay, the reference compounds dexamethasone and RU486 bound with calculated K_d values of 3 nM (IC_{50}, 10 nM; $r^2 = 0.99$) and 15 nM (IC_{50}, 100 nM; $r^2 = 0.98$), respectively (Figs. 1 and 2A). The in vitro measured dexamethasone binding data were consistent with binding data generated in intact THP-1 monocytic cells using radiolabeled dexamethasone as a tracer compound (data not shown). The high-throughput screen of our proprietary compound library led to the identification of GP052499, a compound that represents the steroid cyproterone acetate (Neumann, 1994) (Fig. 1). The GR binding data for cyproterone acetate were fitted to a one binding site equation with a correlation coefficient of 0.92 that yielded a K_d value of 45 nM (IC_{50}, 360 nM) (Fig. 2B).

The PR is highly homologous to the GR and was used to compare the binding selectivity of the steroid ligands (Fig. 1). The PR competitive binding assay uses an amino-terminal glutathione *S*-transferase fusion of the PR LBD and a proprietary fluorescent-tagged progesterone ligand. Progesterone and RU486 revealed similar binding affinities with K_d values of 16 (IC_{50}, 106 nM; $r^2 = 0.97$) and 40 nM (IC_{50}, 307 nM; $r^2 = 0.99$), respectively (Figs. 1 and 2C). Cyproterone acetate bound the progesterone receptor with a K_d value of 15 nM (IC_{50}, 79 nM; $r^2 = 0.98$) (Fig. 2D). In comparison, dexamethasone with a K_d value of 300 nM (IC_{50}, 2.2 μM; $r^2 = 0.99$) for the PR was clearly more selective for GR.

Whole-Cell Functional Assays to Distinguish GR Agonistic from GR Antagonistic Ligand Properties. To characterize further the steroids and their functional potentials, a cellular assay for GR-mediated transcriptional activation was required. The *TAT* gene is liver-specific and glucocorticoid-inducible (Diamondstone, 1966). The GR has been shown to bind to the TAT GRE in vitro and, upon hormone binding, to activate transcription of the TAT gene in vivo. Diamondstone described an assay for TAT activity that is based on the conversion of *p*-hydoxyphenylpyruvic acid to *p*-hydroxybenzaldehyde in strong alkali (Diamondstone, 1966). We adapted the Diamondstone assay concept to a microplate format and showed a dose-dependent induction of TAT activity by dexamethasone in the rat hepatoma cell line H4IIE-C3. To optimally characterize the pharmacological profile of GR binding compounds, the TAT assay was first executed in the Schild format and then in the titration format.

The execution of the cellular assay in the Schild format tested the dose-dependent induction of TAT by dexamethasone in presence or absence of one excessive test compound concentration of 10 μM (Fig. 3, A and B). Hence, a test compound with agonistic activity will shift the dexamethasone dose-response curve upward, whereas a compound with antagonistic activity will shift the dose-response curve of dexamethasone to the right. RU486 revealed no intrinsic agonistic activity yet completely repressed the transactivating activity of dexamethasone in H4IIE-C3 cells (Fig. 3A). The dose-dependent activation of TAT activity by dexamethasone was measured at an EC_{50} value ($n = 4$) of 1.8 ± 1.0 nM (S.D.) with a coefficient of correlation of 0.97 ± 0.01 (S.D.). A 10-fold excess of RU486 (10 μM) over dexamethasone (1 μM) was sufficient to antagonize transactivation ($p \leq 0.001$). Similar to RU486, cyproterone acetate revealed no ability to intrinsically transactivate the GR (Fig. 3B). However, unlike

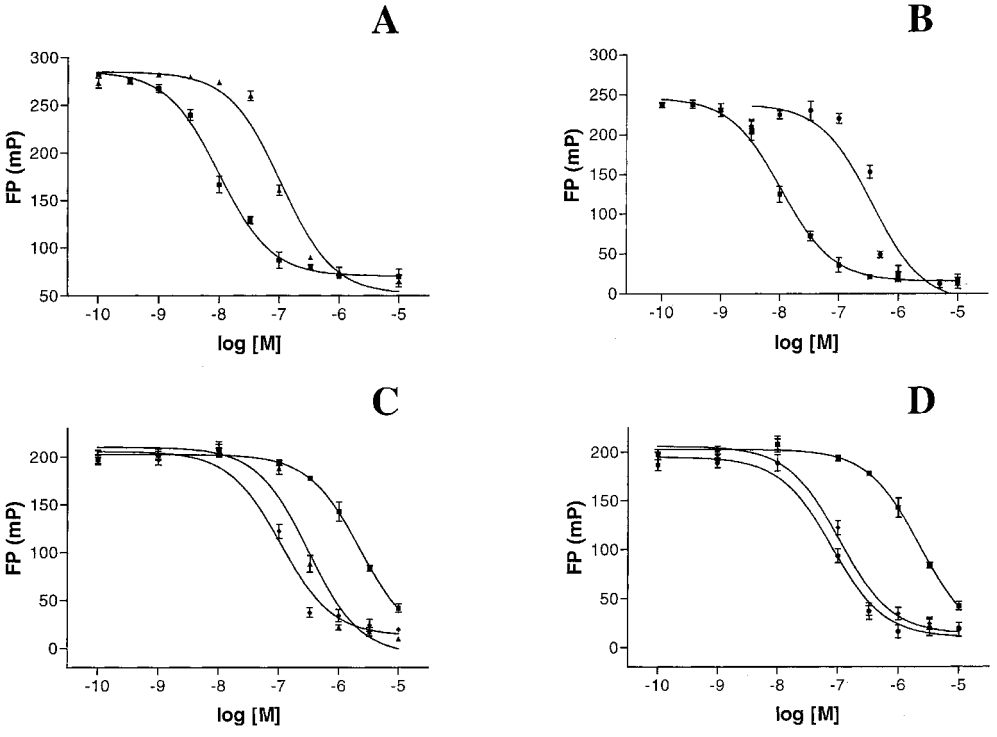

Fig. 2. Determination of steroid receptor binding in vitro. A and B, dose-dependent displacement of fluormone-GS1 from GR binding by steroid ligands. The binding equilibrium of fluormone-GS1/test compound to the GR preparation was assessed by FP measurement. The binding data were fitted to a one binding site equation that yielded a K_d of 3 nM ($r^2 = 0.99$) for dexamethasone (■), 15 nM for RU486 ($r^2 = 0.97$) (▲), and 45 nM ($r^2 = 0.92$) for cyproterone acetate (●). C and D, dose-dependent displacement of fluormone-PL green from the PR by steroid ligands. The binding equilibrium of fluormone-PL to the PR preparation was assessed by FP after 2 h. The binding data were fitted to a one binding site equation that yielded a K_d of 16 nM ($r^2 = 0.97$) for progesterone (♦), 40 nM ($r^2 = 0.96$) for RU486 (▲), 300 nM ($r^2 = 0.99$) for dexamethasone (■), and 15 nM ($r^2 = 0.98$) for cyproterone acetate (●).

RU486, a 10-fold excess of cyproterone acetate over dexamethasone was insufficient to suppress TAT expression; 100-fold excess yielded a complete suppression ($p \leq 0.001$). Therefore, the antagonistic potency of cyproterone acetate is, comparison with that of RU486, approximately 1 order of magnitude lower.

The execution of the cellular assay in the titration format tested the dose-dependent ability of test compounds to inhibit the dexamethasone-induced activity of TAT (Fig. 3, C and D). Both RU486 and cyproterone acetate dose-dependently repressed the submaximal TAT activity induced by dexamethasone at a 5-fold EC_{50} concentration. An EC_{50} value of 1.8 ± 1.0 nM was calculated for dexamethasone by nonlinear regression analysis ($r^2 = 0.97 \pm 0.01$) (Fig. 3, A and B). The dose-dependent competition curve for RU486 yielded a K_i value of 10 nM (IC_{50}, = 43; $r^2 = 0.94$) (Fig. 3C). The calculated K_i value of 30 nM for cyproterone acetate was slightly lower than for RU486 (IC_{50}, = 150 nM; $r^2 = 0.97$) (Fig. 3D).

To test the GR antagonism of these compounds in a different cellular background, a dexamethasone-controlled transient GRE reporter gene assay was established in MG-63 osteosarcoma cells. Dexamethasone caused a dose-dependent increase in luciferase expression; 5 nM dexamethasone yielded a half-maximal response, and 30 nM resulted in a maximal induction (11-fold) of luciferase activity (EC_{50}, 1.4 nM; $r^2 = 0.99$) (Fig. 4A). Neither cyproterone acetate nor RU486 exhibited luciferase-inducing activity at concentrations up to 10 μM (data not shown). However, both compounds blocked the transactivational response to dexamethasone in a concentration-dependent manner (Fig. 4, A and B). The presence of 10 nM RU486 shifted the dose-response curve of dexamethasone by approximately 1 order of magnitude to the right, whereas the presence of 100 nM RU486 abolished the ability of dexamethasone to transactivate the reporter gene (Fig. 4A). In comparison, a cyproterone acetate concentration of 1 μM was necessary to significantly shift the dexamethasone dose-response curve to the right and a concentration of 10 μM was required to abolish the dexamethasone-induced reporter gene activity (Fig. 4B). Therefore, cyproterone acetate was approximately 100-fold less potent than RU486 to compete with dexamethasone for reporter gene transactivation.

To further characterize the antagonistic properties of RU486 and cyproterone acetate in MG63 osteosarcoma cells, the effect of these compounds on glucocorticoid-mediated transrepression of cytokine release was assessed. Dexamethasone abolished dose dependently in MG63 cells the IL-1β induced production of IL-6; 0.3 and 30 nM dexamethasone resulted in 50 and >90% inhibition of cellular IL-6 release, respectively (Fig. 4C). Neither RU486 nor cyproterone acetate at concentrations up to 10 μM inhibited IL-6 production (data not shown). However, both compounds dose dependently affected the inhibitory activity of dexamethasone by shifting the dose-response curve of dexamethasone to the right (Fig. 4, C and D). Unlike the antagonism of the transactivational response to dexamethasone, the highest concentrations of RU486 (100 nM) and cyproterone acetate (10 μM) were only able to partially reverse the transrepressional activity induced by 100 nM dexamethasone. Similar results were observed using human dermal and synovial fibroblasts (data not shown).

In Vivo Target Pharmacology. The ability to measure TAT activity from partially purified enzyme preparations was subsequently used for the development of a tissue selective in vivo biomarker for GR modulation. The procedure to measure TAT activity in cells was adapted to determine activity in isolated rat liver tissue (Hayashi et al., 1967; Granner and Tomkins, 1970). The assessment of TAT activity in the rat livers upon oral administration of a test compound is reflective of the compound's oral bioavailability and pharmacodynamic activity profile.

Optimal dexamethasone concentrations and treatment

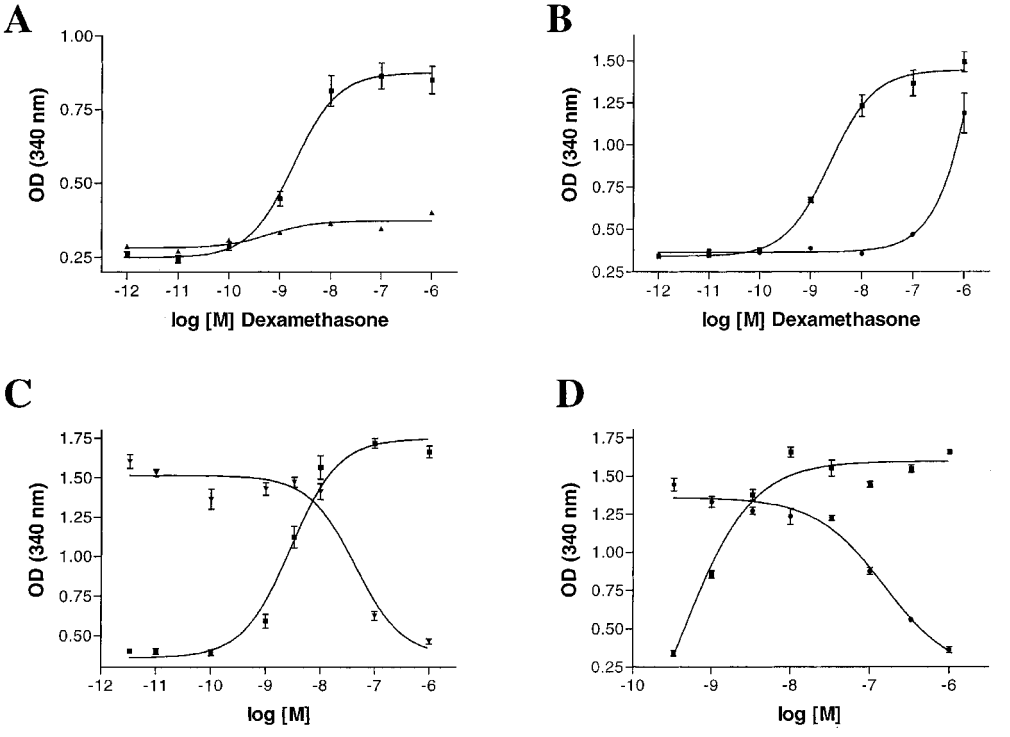

Fig. 3. Determination of GR-mediated transcriptional activation of TAT in H4IIE-C3 cells. A and B, the H4IIE-C3 TAT assay in the Schild format. A dexamethasone dose-response curve in presence or absence of excess RU486 (A) or cyproterone acetate (B). In absence of competing compounds, dexamethasone induced activation of TAT is fitted to a one binding site receptor model with a correlation coefficient of $r^2 = 0.97 \pm 0.01$ yielding an EC_{50} of 1.8 ± 1.0 nM (■). C and D, the H4IIE-C3 TAT assay in the titration format. Dose-dependent inhibition of dexamethasone-induced TAT activity by RU486 (▲) and cyproterone acetate (●). The applied dexamethasone concentration corresponded to the 5-fold EC_{50} value determined in a dose-TAT induction curve (■). The competition data were fitted to a one binding site receptor equation that yielded a K_i of 10 nM ($r^2 = 0.94$) for RU486 and a K_i of 30 nM for cyproterone acetate ($r^2 = 0.97$).

times for hepatic induction of TAT activity were determined in independent experiments. A dexamethasone dose-response study was performed by i.p. administration of various doses of dexamethasone to Sprague-Dawley rats (Fig. 5A). The animals were sacrificed 3 h after injections, and a dose-dependent induction of liver TAT activity by dexamethasone over vehicle control treatment was observed. The maximal TAT activity was obtained with 0.01 mg/kg dexamethasone ($p \leq 0.05$). The time-response study was performed by i.p. administration of dexamethasone at 0.03 mg/kg or vehicle control and the isolation of liver tissue at various time points (Fig. 5B). One hour after dexamethasone administration, no significant induction of hepatic TAT activity was observed. However, 3 and 5 h after treatment, a significant dexamethasone-induced increase of TAT activity was recorded. The TAT activity increased 2.1-fold at 3 h ($p \leq 0.01$) and 2.5-fold at 5 h ($p \leq 0.01$) after dexamethasone administration.

To assess the reversibility of the dexamethasone-induced and GR-mediated TAT activity, a competition study was performed with the coadministration of RU486 or cyproterone acetate (Fig. 5, C and D). The GR antagonists were administered orally by gavage at 40 mg/kg and 80 mg/kg rat body weight and 10 min before the i.p. injection of dexamethasone at 0.01 mg/kg. Four hours after the injections, the rats were sacrificed and the isolated livers subjected to the TAT assay. The experiment was stress controlled by the administration of vehicle, both oral and i.p., and compared with untreated rats. The dexamethasone treatment resulted in a 1.9-fold increase of TAT activity ($p \leq 0.05$) that was completely prevented by the oral administration of RU486 ($p \leq 0.01$). Cyproterone acetate proved to be active in vivo albeit with weaker potency than RU486. The dexamethasone treatment resulted in a 3.2-fold increase of TAT activity ($p \leq 0.001$) that was significantly suppressed by *Cyproterone acetate* ($p \leq 0.05$), albeit to a lesser extent than by RU486. The injections and gavage treatment resulted in minimal stress with insignificant impact on TAT activity. Therefore, the assessment of hepatic TAT activity served as a pharmacological marker for the specific modulation of the GR in vivo upon oral administration of test compounds.

Pharmacophore Modeling using a GR Homology Model. A homology model was created for the LBD of GR based on the X-ray crystal structure of the progesterone bound LBD of PR (Williams and Sigler, 1998). The GR and PR LBD sequences share 53% identity and 74% homology. In particular, the pocket regions for hormone binding show high sequence conservation between PR and GR. Within a shell of 5 Å around the progesterone-bound PR pocket, only five residues are altered in GR: L715M, V760A, F794Q, L797Q, and M909L (numbers indicate amino acid residues in PR). In the reported nuclear receptor structures, steroid hormones with a core template consisting of the A, B, C, and D rings dock in a common orientation with the A rings oriented toward a conserved arginine residue from helix 5 and the D rings toward the AF-2 helix. The polar substituents in steroid hormones are mainly located at position C3 on the A ring and C17 on the D ring. The natural ligands, progesterone for the PR and cortisol for the GR, differ by the occurrence of three additional hydroxyl groups in cortisol (Fig. 1). The L797Q mutation between PR and GR may explain the preferential binding of cortisol by GR that features at position C17α a hydroxyl moiety.

Cyproterone acetate was docked into the GR homology model using a LMOD conformational search algorithm (Fig. 6A). The carbonyl group in the C3 position of cyproterone acetate engaged in a hydrogen bond to the guanidinium of R611 and to the γ-amide of Q570. The carbonyl group on C20α of cyproterone acetate bonded with residue T739 in the GR binding pocket. These interactions are also recognized by dexamethasone as shown in the crystal structure of the GR-

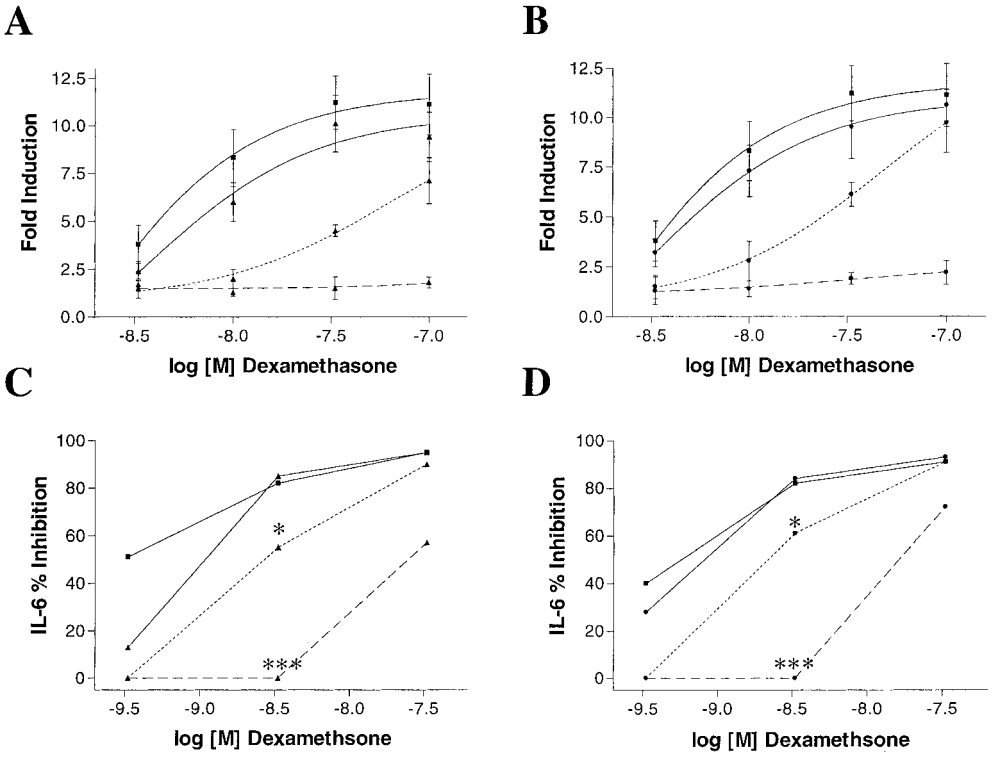

Fig. 4. GR-mediated transactivation and transrepression in MG63 osteosarcoma cells. A and B, dose-response curve of dexamethasone in MG-63 cells transiently transfected with a pGRE-luciferase reporter gene construct in the presence or absence of RU486 (A) and cyproterone acetate (B). The GRE promotor activity was normalized in presence of vehicle. A, dexamethasone in the absence of compound (EC_{50}, 1.4 nM; $r^2 = 0.99$) (■) and in presence of RU486 at 1 nM (—▲—), 10 nM (- -▲- -), or 100 nM (– –▲– –). B, dexamethasone in absence of compound (■) and in presence of cyproterone acetate at 100 nM (—●—), 1,000 nM (- -●- -) or 10,000 nM (– –●– –). The results are the average (± S.D.) for six determinations pooled from two experiments. C and D, dose-response curve of dexamethasone in MG-63 cells on IL-1β–induced IL-6 release in presence or absence of RU486 (C) and cyproterone acetate (D). The IL-6 release was normalized in presence of vehicle. C, dexamethasone in presence of vehicle (■) and in presence of RU486 at 1 nM (—▲—), 10 nM (- -▲- -) or 100 nM (– –▲– –). B, dexamethasone in presence of vehicle (■) and in presence of cyproterone acetate at 100 nM (—●—), 1000 nM (- -●- -), or 10,000 nM (– –●– –). The results are the average ± S.D. for two experiments

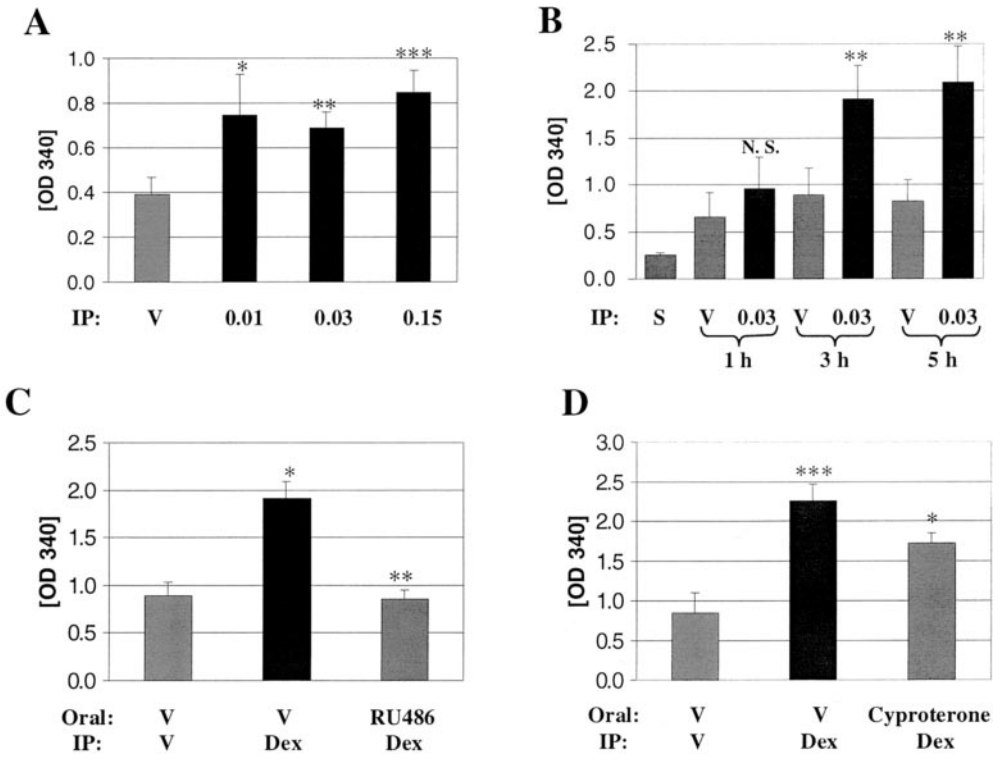

Fig. 5. Determination of GR-mediated transcriptional activation of TAT in vivo. Sprague-Dawley rats were subjected to various treatments and the livers were harvested for TAT activity determination. A, dexamethasone dose-response study. The animals were injected i.p. with vehicle (V) or increasing doses of dexamethasone as indicated, and livers were harvested 3 h later for TAT activity assessment. Data are represented as mean ± S.D. B, dexamethasone time-response study. The animals were injected i.p. with vehicle (V) or 0.03 mg/kg dexamethasone, and livers were harvested after various time points as indicated for TAT activity determination. The assessment of untreated animals was used as stress control (S). Data are represented as mean ± S.D. C and D, competitive study. Treatment groups consisting each of four animals are represented by mean ± S.D. Vehicle-vehicle control group, animals were subjected to oral gavage with vehicle (V) followed by an i.p. injection of vehicle (V). Vehicle-dexamethasone group, animals were subjected to oral gavage with vehicle (V) followed by an i.p. injection of dexamethasone at 0.01 mg/kg (Dex). GR antagonist-dexamethasone group: animals were subjected to oral gavage with RU486 at 40 mg/kg (RU486) or cyproterone acetate at 80 mg/kg (Cyproterone) followed by an i.p. injection of dexamethasone at 0.01 mg/kg (Dex).

dexamethasone complex by Bledsoe et al. (2002). The acetyl group at C17β position on the D ring of cyproterone, however, did not reveal any recognizable hydrophilic interactions with a nearby residue, such as Q642, despite the allowance of full conformational docking flexibility.

Docking of RU486 into the GR homology model showed a similar positioning of the steroid scaffold with the carbonyl group in the C3 position, forming a hydrogen bond to the guanidinium of R611 and to the γ-amide of Q570 (Fig. 6B). The dimethylaminophenyl side chain at position C11β on the C ring of RU486 projected toward the protein surface to displace the AF-2 helix from its active conformation. This molecular mode of receptor antagonism has been previously shown for 4-hydroxytamoxifen complexed to the ER (Protein Data Base code 3ERT) (Shiau et al., 1998). Overlaying cyproterone acetate with RU486 in the GR binding pocket clearly demonstrated the absence of a protruding bulky side chain in cyproterone acetate that may cause a reposition of the AF-2 helix (Fig. 6B). Therefore, based on the molecular docking of these steroids to the GR homology model, the antagonistic properties of cyproterone acetate may occur by a molecular mechanism that is different from the mechanism ascribed to RU486.

Discussion

In this report, we present a new pharmacological profile of cyproterone acetate. Cyproterone acetate competitively abolished GR transactivation by dexamethasone in vitro and in vivo upon oral administration to rats. The GR activity profile

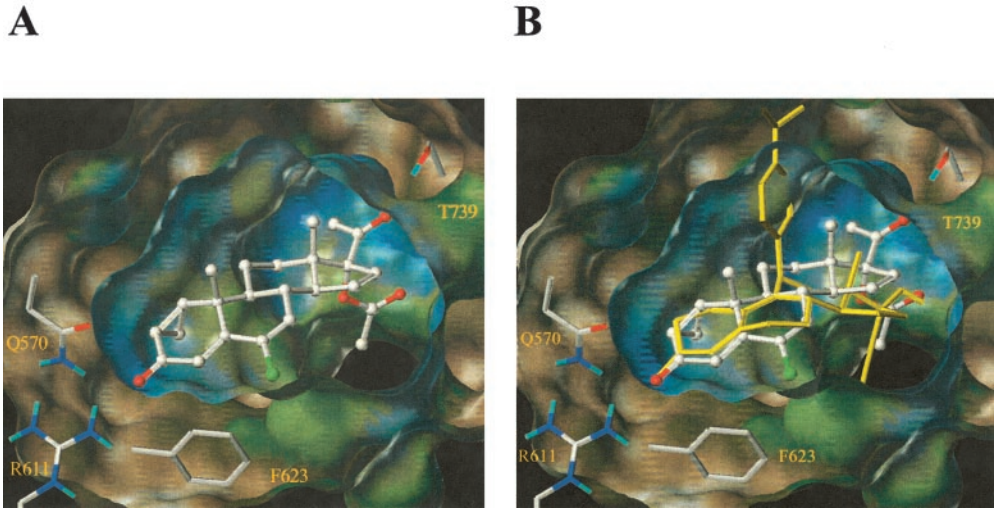

Fig. 6. Structural determination of GR antagonism in silico. A, docking of the cyproterone acetate structure into the GR homology model. The GR model was built on the template given by X-ray crystal structure for the active conformation of progesterone-bound PR (Protein Data Bank code 1A28). The C3 carbonyl group of cyproterone formed a hydrogen bond with the side-chains of R611 and Q570. The C20α of cyproterone acetate formed a hydrogen bond with the hydroxyl group of the T739 side chain. B, coordinated overlay of the docking models for cyproterone acetate (in white) and RU486 (in yellow) in the GR homology model. The cyproterone acetate docked receptor surface was used for the overlay of RU486.

of cyproterone acetate in our assays was comparable with that of RU486; however, the potency of cyproterone acetate was inferior to that of RU486. Interestingly, the apparent potency of both compounds to antagonize dexamethasone-induced GR transactivation was better than their ability to prevent dexamethasone-mediated transrepression of cellular cytokine release. This observation may indicate differential kinetics or mechanisms for GR ligands to control GRE- and NFκB-dependent transactivation. Alternatively, this observation may reflect the higher intrinsic potency of dexamethasone for transrepression than for transactivation.

Cyproterone acetate has orphan drug status in the United States and is used as antiandrogen in other countries. The steroid has been shown to compete with dihydrotestosterone for binding to the androgen receptor and to exhibit progestogenic activities. Indeed, progesterone itself is a weak antiandrogen. Cyproterone also suppresses the secretion of gonadotropins and thus interferes with testosterone production (Barradell and Faulds, 1994; Neumann, 1994). The agent is used for the treatment of paraphilias and inoperable prostate cancer in men. In women, cyproterone is used for the treatment of acne or virilizing syndromes such as hirsutism and combined with estrogens as hormone replacement therapy and contraception (van Wayjen and van den Ende, 1995; Morin-Papunen et al., 2000; Borissova et al., 2002). A rare association with severe liver damage and hepatocellular carcinoma, however, limits the usefulness of cyproterone acetate.

The drug label also indicates a potential change in glucose tolerance and thus a possible interaction with antidiabetic drugs. The metabolic homeostasis is determined by the secretion of glucoregulatory hormones, including insulin, glucagon, epinephrine, growth hormone, and cortisol. Cortisol may increase plasma glucose concentrations by stimulating appetite and hepatic gluconeogenesis. Therefore, inhibition of the GR with cyproterone acetate may affect the peripheral glucose metabolism, the stress response, and the regulation of the hypothalamic pituitary axis.

The recent elucidation of the long-awaited crystal structure of the GR along with the proposed molecular mechanisms for activation and repression of nuclear receptors generated a new basis for the structural interpretation of the biological activities mediated by GR ligands such as cyproterone acetate. Crystal structures of several nuclear receptors demonstrated that the selectivity of steroid hormone binding is achieved by the complementarity of shape and hydrogen bonding between ligands and the receptor ligand binding pockets. Thus, the high affinity of dexamethasone for the GR was readily explained by the extensive network of hydrophobic and hydrophilic interactions between the ligand and the protein (Bledsoe et al., 2002). Ligands with the ability to transactivate their receptor have been shown to shift the conformational equilibrium to an active conformation such that the AF-2–mediating helix takes a position that increases the affinity of the LBD for coactivators. Indeed, dexamethasone makes direct contacts between the C21 hydroxyl group and L753 in the AF-2 helix and between the C11β hydroxyl group and residue I747 in the loop preceding the AF-2 helix. These interactions are likely to stabilize the AF-2 helix in an active conformation and may serve as a molecular basis for ligand-dependent activation of GR. These hydroxyl groups are conserved in cortisol yet are lacking in cyproterone acetate that may explain its inability to transactivate the GR.

The molecular mechanism for "active antagonism" of nuclear receptors has been explained by the projection of bulky side chains that block the AF-2 activity. RU486 contains such a side chain at position C11β on the C ring that protrudes out of the binding pocket, thereby preventing the AF-2 helix from adopting an active conformation and shifting the LBD affinity from coactivator to corepressor recruitment. Because cyproterone acetate lacks a bulky side chain similar to RU486, the observed functional effects of cyproterone acetate may occur by a different mode of receptor antagonism. Recently, a similar deviation from the classic nuclear receptor antagonist model has been made with the ERβ antagonist compound THC (Shiau et al., 2002). THC lacks a bulky side chain, and the crystal structure of the THC-ERβ complex did not reveal any steric hindrance of the AF-2 helix. In this model, THC antagonized ERβ by stabilizing nonproductive conformations of key residues in the ligand-binding pocket. The authors referred to this molecular mode as "passive antagonism". Theoretically, cyproterone acetate may induce a similar mode of passive antagonism by shifting the stability equilibrium in favor of an inactive receptor conformation. Indeed, we observed a differential shift in the GR binding affinity for cyproterone and RU486 in presence or absence of a coactivator peptide (supplementary data). The binding affinity for cyproterone increased in presence of coactivator peptide in contrast to RU486, the binding affinity of which decreased. The addition of coactivator peptide had no effect on the binding affinity of dexamethasone or cortisol. The observed antagonism of both dexamethasone-induced TAT activation and blockage of IL-6 release by cyproterone may therefore occur by competitive displacement of dexamethasone from the GR binding pocket to reach a new stability equilibrium. Competitive displacement by locking a nuclear receptor in an inactive conformation would also explain the mineralocorticoid and androgen receptor antagonism by progesterone and drospirenone (Souque et al., 1995; Singh et al., 2000). By designing compounds that selectively stabilize inactive conformations in certain nuclear receptors and active conformations in others, new therapeutic benefits can be achieved.

The introduction of I628A mutation in the LBD of GR has been shown to impair receptor dimerization and the ability to mediate transactivation while retaining the ability to transrepress NF-κB activated functions (Bledsoe et al., 2002). The dimerization defective mutant GR^{dim} mouse exhibited a similar phenotype characterized by affected transactivation and unaffected transrepression abilities (Reichardt et al., 1998; Tronche et al., 1998). The design of selective GR modulating compounds that inhibit transactivation while retaining transrepression may therefore occur on the basis of chemical scaffolds that mediate passive receptor antagonism and interference in the receptor dimerization properties.

Acknowledgments

We thank Carrol Berry, Xin Wang, and Beverly Battle for excellent technical assistance. We are also grateful to Shari Caplan and James Stanton for critically reading the manuscript.

References

Barradell LB and Faulds D (1994) Cyproterone. A review of its pharmacology and therapeutic efficacy in prostate cancer. *Drugs Aging* **5:**59–80.

Bledsoe R, Montana V, Stanley TB, Delves CJ, Apolito CJ, McKee DD, Consler TG, Parks DJ, Stewart EL, Willson TM, et al. (2002) Crystal structure of the glucocorticoid receptor ligand binding domain reveals a novel mode of receptor dimerization and coactivator recognition. *Cell* **110:**93–105.

Borissova AM, Tankova T, Kamenova P, Dakovska L, Kovacheva R, Kirilov G, Genov N, Milcheva B, and Koev D (2002) Effect of hormone replacement therapy on insulin secretion and insulin sensitivity in postmenopausal diabetic women. *Gynecol Endocrinol* **16:**67–74.

Bourguet W, Germain P, and Gronemeyer H (2000) Nuclear receptor ligand-binding domains: three-dimensional structures, molecular interactions and pharmacological implications. *Trends Pharmacol Sci* **21:**381–388.

Bourguet W, Ruff M, Chambon P, Gronemeyer H, and Moras D (1995) Crystal structure of the ligand-binding domain of the human nuclear receptor RXR-alpha. *Nature (Lond)* **375:**377–382.

Brzozowski AM, Pike AC, Dauter Z, Hubbard RE, Bonn T, Engstrom O, Ohman L, Greene GL, Gustafsson JA, and Carlquist M (1997) Molecular basis of agonism and antagonism in the oestrogen receptor. *Nature (Lond)* **389:**753–758.

Cadepond F, Ulmann A, and Baulieu EE (1997) RU486 (mifepristone): mechanisms of action and clinical uses. *Annu Rev Med* **48:**129–156.

Chen JD and Evans RM (1995) A transcriptional co-repressor that interacts with nuclear hormone receptors. *Nature (Lond)* **377:**454–457.

Cheng Y and Prusoff WH (1973) Relationship between the inhibition constant (K1) and the concentration of inhibitor which causes 50 per cent inhibition (I50) of an enzymatic reaction. *Biochem Pharmacol* **22:**3099–3108.

Diamondstone T (1966) Assay of tyrosine transaminase activity by conversion of p-hydroxyphenylpyruvate to *p*-hydroxybenzaldehyde. *Anal Biochem* **16:**395–401.

Granner D and Tomkins G (1970) Tyrosine aminotransferase (rat liver). *Methods Enzymol* **17A:**633–670.

Glass CK and Rosenfeld MG (2000) The coregulator exchange in transcriptional functions of nuclear receptors. *Genes Dev* **14:**121–141.

Gronemeyer H, Benhamou B, Berry M, Bocquel MT, Gofflo D, Garcia T, Lerouge T, Metzger D, Meyer ME, Tora L, et al. (1992) Mechanisms of antihormone action. *J Steroid Biochem Mol Biol* **41:**217–221.

Hayashi SI, Granner DK, and Tomkins GM (1967) Tyrosine aminotransferase. Purificaton and characterization. *J Biol Chem* **242:**3998–4006.

Karin M (1998) New twists in gene regulation by glucocorticoid receptor: is DNA binding dispensable? *Cell* **93:**487–490.

Kolossvary I and Guida WC (1996) Low mode search. An efficient, automated computational method for conformational analysis: application to cyclic and acyclic alkanes and cyclic peptides. *J Am Chem Soc* **118:**5011–5019.

Kolossvary I and Guida WC (1999) Low-mode conformational search elucidated. Application to C39H80 and flexible docking of 9-deazaguanine inhibitors to PNP. *J Comput Chem* **20:**1671.

McKenna NJ, Lanz RB, and O'Malley BW (1999) Nuclear receptor coregulators: cellular and molecular biology. *Endocr Rev* **20:**321–344.

Morin-Papunen LC, Vauhkonen I, Koivunen RM, Ruokonen A, Martikainen HK, and Tapanainen JS (2000) Endocrine and metabolic effects of metformin versus ethinyl estradiol-cyproterone acetate in obese women with polycystic ovary syndrome: a randomized study. *J Clin Endocrinol Metab* **85:**3161–3168.

Neumann F (1994) The antiandrogen cyproterone acetate: discovery, chemistry, basic pharmacology, clinical use and tool in basic research. *Exp Clin Endocrinol* **102:**1–32.

Philibert D and Teutsch G (1990) RU 486 development. *Science (Wash DC)* **247:**622.

Reichardt HM, Kaestner KH, Tuckermann J, Kretz O, Wessely O, Bock R, Gass P, Schmid W, Herrlich P, Angel P, et al. (1998) DNA binding of the glucocorticoid receptor is not essential for survival. *Cell* **93:**531–541.

Renaud JP, Rochel N, Ruff M, Vivat V, Chambon P, Gronemeyer H, and Moras D (1995) Crystal structure of the RAR-gamma ligand-binding domain bound to all-trans retinoic acid. *Nature (Lond)* **378:**681–689.

Sack JS, Kish KF, Wang C, Attar RM, Kiefer SE, An Y, Wu GY, Scheffler JE, Salvati ME, Krystek SR Jr, et al. (2001) Crystallographic structures of the ligand-binding domains of the androgen receptor and its T877A mutant complexed with the natural agonist dihydrotestosterone. *Proc Natl Acad Sci USA* **98:**4904–4909.

Sapolsky RM, Romero LM, and Munck AU (2000) How do glucocorticoids influence stress responses? Integrating permissive, suppressive, stimulatory and preparative actions. *Endocr Rev* **21:**55–89.

Shiau AK, Barstad D, Loria PM, Cheng L, Kushner PJ, Agard DA, and Greene GL (1998) The structural basis of estrogen receptor/coactivator recognition and the antagonism of this interaction by tamoxifen. *Cell* **95:**927–937.

Shiau AK, Barstad D, Radek JT, Meyers MJ, Nettles KW, Katzenellenbogen BS, Katzenellenbogen JA, Agard DA, and Greene GL (2002) Structural characterization of a subtype-selective ligand reveals a novel mode of estrogen receptor antagonism. *Nat Struct Biol* **9:**359–364.

Singh SM, Gauthier S, and Labrie F (2000) Androgen receptor antagonists (antiandrogens): structure-activity relationships. *Curr Med Chem* **7:**211–247.

Souque A, Fagart J, Couette B, Davioud E, Sobrio F, Marquet A, and Rafestin-Oblin ME (1995) The mineralocorticoid activity of progesterone derivatives depends on the nature of the C18 substituent. *Endocrinology* **136:**5651–5658.

Srinivasan G and Thompson EB (1990) Overexpression of full-length human glucocorticoid receptor in Spodoptera frugiperda cells using the baculovirus expression vector system. *Mol Endocrinol* **4:**209–216.

Teutsch G, Gaillard-Moguilewsky M, Lemoine G, Nique F, and Philibert D (1991) Design of ligands for the glucocorticoid and progestin receptors. *Biochem Soc Trans* **19:**901–908.

Tronche F, Kellendonk C, Reichardt HM, and Schutz G (1998) Genetic dissection of glucocorticoid receptor function in mice. *Curr Opin Genet Dev* **8:**532–538.

van Wayjen RG and van den Ende A (1995) Experience in the long-term treatment of patients with hirsutism and/or acne with cyproterone acetate-containing preparations: efficacy, metabolic and endocrine effects. *Exp Clin Endocrinol Diabetes* **103:**241–251.

Wagner RL, Apriletti JW, McGrath ME, West BL, Baxter JD, and Fletterick RJ (1995) A structural role for hormone in the thyroid hormone receptor. *Nature (Lond)* **378:**690–697.

Williams SP and Sigler PB (1998) Atomic structure of progesterone complexed with its receptor. *Nature (Lond)* **393:**392–396.

Address correspondence to: Christoph Schumacher, Ph.D., Speedel Holding AG, Hirschgasslein 11, 4051 Basel, Switzerland. E-mail: christoph.schumacher@speedelgroup.com